
This is the accepted manuscript version of the article

Hot-Box measurements of highly insulated wall, roof and floor structures

Gullbrekken, L., Uvslokk, S., Kvande, T., & Time, B.

Citation for the published version (APA 6th)

Gullbrekken, L., Uvslokk, S., Kvande, T., & Time, B. (2017). Hot-Box measurements of highly insulated wall, roof and floor structures. *Journal of Building Physics*, 41(1), 58-77.
doi:10.1177/1744259116669516

This is accepted manuscript version.

It may contain differences from the journal's pdf version.

This file was downloaded from SINTEFs Open Archive, the institutional repository at SINTEF

<http://brage.bibsys.no/sintef>

Hot-Box measurements of highly insulated wall, roof and floor structures

Abstract

The purpose of this study was to investigate how natural convection in air permeable glass wool insulation affects the thermal transmittance in walls, roofs and floor structures. The results can be used to evaluate the need for a convection barrier in thick mineral wool layers. Natural convection is affected by several parameters. In this study, the angle of inclination, the heat flow direction and the temperature difference across the test section have been studied. Thermal transmittance and temperature distribution measured by use of thermocouples placed inside the insulation cavity clearly showed convection in the insulation when the test section was in pitched roof and wall positions. An efficient measure to reduce the natural convection is to divide the insulation layer into two thinner layers by using a diffusion open convection barrier. A convection barrier is recommended by the authors both in wall and pitched roof structures if the insulation thickness exceeds 200 mm.

Keywords

Laboratory measurements, Hot-Box, natural convection, heat transfer, insulation

Introduction

Convection in building structures

Convection, or air flow, in building structures is caused by pressure differences from driving forces like fans, wind and temperature differences. Resulting air flow caused by temperature differences is called natural convection. The driving force is buoyancy caused by density differences in the air because of the temperature differences.

The risk of natural convection in an enclosure filled with a permeable material exposed to a given temperature difference may be described by the modified Rayleigh number Ra^* . Ra^* is defined in NS-EN ISO 10456 (2007), see equation (1). According to NS-EN ISO 10456 (2007), natural convection can be neglected when calculating U-values if $Ra^* < 2.5$.

$$Ra^* = \frac{g \beta \rho c_p}{\nu} \frac{dk \Delta T}{\lambda_m} \quad (1)$$

The properties of the air are the heat expansion coefficient; β (1/K), kinematic viscosity; ν (m²/s), density; ρ (kg/m³), and specific heat capacity; c_p (J/kg K). The

properties of the insulation material are air permeability; k (m^2), and thermal conductivity; λ_m ($\text{W}/\text{m}^2\text{K}$). ΔT is the temperature difference across the specimen with insulation thickness, d (m).

The permeability of the mineral wool, k (m^2), given in equation (1) was calculated according to the following equation:

$$k = \frac{L \cdot v \cdot dx}{A \cdot \Delta P} \quad (2)$$

, L is the air flow (m^3/s), v is the kinematic viscosity (m^2/s), dx is the insulation thickness (m), A is the crosssectional area which air is flowing through (m^2), ΔP is the pressure difference (Pa).

However, the fibre orientation in glass wool battens is not evenly distributed, but dominated by fibres parallel to the batten surface. Because of this, the permeability is usually substantially larger parallel (\parallel) rather than perpendicular (\perp) to the batten surface (Marmolet et al., 2012). To account for this, an equivalent permeability, k_e (m^2), representative for the air flow path, should be estimated and used in equation (1). According to Uvsløkk et al. (1996), k_e for walls can be calculated using the equation (3). The equation takes into account the difference in permeability perpendicular to and parallel to the main fibre orientation, the cross-section area and length of a simplified flow path in the insulated cavities.

$$k_e = \frac{\frac{h}{d} + \frac{d}{h}}{\frac{h}{d \cdot B_{\parallel}} + \frac{d}{h \cdot B_{\perp}}} \quad (3)$$

where h is the height of the insulated wall cavity (m), d is the depth (thickness) of the wall insulation (m), B_{\parallel} is the permeability parallel to the fibres (m^2), and B_{\perp} is the permeability perpendicular to the fibres (m^2).

Of interest when evaluating the thermal performance of structural components is also the ratio of the total heat transfer including convection to heat transfer without convection. The ratio is given by the Nusselt number, Nu , and has been calculated according to the following equation:

$$Nu = \frac{U}{U_0} \quad (4)$$

U is the U-value measured in the Hot-Box ($\text{W}/\text{m}^2\text{K}$) and U_0 is the U-value when there is no convection ($\text{W}/\text{m}^2\text{K}$). In the present Hot-Box measurement the U_0 is the value of the tested structure in horizontal floor configuration, with heat flow direction downwards).

Challenges in structures with thick insulation

Buildings that are designed to meet high energy performance requirements, e.g. passive houses, require well-insulated building envelopes, with increased insulation thicknesses for roof, wall and floor structures. Increased insulation thicknesses may lead to increased risk of mould growth and moisture damage (Økland, 1998; Gullbrekken et al., 2015). One reason for this is increased risk of natural convection in the insulated cavities causing moisture redistribution in the timber frame.

Natural convection will cause the air to circulate in the cavity, rise on the warm side and drop on the cold side. The amount of natural convection depends on the driving forces and the flow resistance of the insulated cavities: 1) temperature difference across the wall, 2) equivalent air permeability of the insulated cavity, and 3) insulation thickness.

In order to avoid convection, it is important that the insulation material fills the cavities completely, especially at the top and bottom of the cavities, in order to avoid air gaps. Gaps will decrease the flow resistance of the insulated cavity and hence increase the convection (Geving, 2011). If the insulation thickness exceeds 200 mm, Uvsløkk et al. (2010) recommend dividing the insulation into two parallel “cavities” using an airtight and vapour open barrier in the middle of two insulation layers. By using this approach, the driving force, the temperature difference across each layer, will be reduced by 50% and the total flow resistance in each layer will be nearly doubled (Uvsløkk et al., 2010).

Convection and the effect on thermal performance

Also previous studies have researched natural convection and effect on thermal performance for wall and roof structures.

Walls

Calculations and measurements performed by Bankvall (1972) indicated that natural convection did not have a significant effect on heat transfer in walls and roofs when glass wool insulation was used. However, the insulation thicknesses in Bankvall’s studies varied from 50 mm to 145 mm and the temperature difference was 10 to 45 K. These insulation layers were rather thin compared with modern Nordic wooden frame structures.

Lecompte (1990) performed calculations of convection through the insulation and around the insulation in a cavity and compared it to Hot-Box measurements. The study only included a wall with 50 mm insulation in a cavity of 80 mm.

Brown et al. (1993) performed an extensive investigation on full-scale laboratory test walls in order to investigate how minor insulation defects affect the surface-averaged thermal resistance. In total, three different insulation densities and three different types of defects were tested. The study indicated that even though the defects were only located in the corners, it affected the natural convection of the entire test wall. Large temperature differences across the test walls and low insulation densities decreased the thermal resistance.

In the mid-1990s, several measurements of large-scale sections of timber frame walls insulated with glass wool were performed in the Hot-Box apparatus at SINTEF Building and Infrastructure/NTNU (Bjerkevoll, 1994; Johannessen, 1995; Jordanger, 1995). All the measurements were performed at standard conditions according to NS-EN-

ISO 8990 (1996). The work was performed in order to study natural convection in real timber frame walls. The wall thickness, type of glass wool and temperature conditions were varied. Some of the results were reported by Uvsløkk et al. (1996). The convection measurements in glass wool were summarized and supplemented by Janssen (1997). These measurements on full-size walls showed experimental Nusselt numbers between 1.07 and 1.12 for a wall with 200 mm glass wool insulation dependent on the temperature difference across the wall. A Nusselt number of 1.07 means that the U-value of a wall with convection is 7% higher than the U-value with no convection. The 300 mm insulated wall gave Nusselt numbers between 1.04 and 1.14. Calculations predicted insignificant amounts of additional heat loss by internal natural convection. A hypothesis of border regions of higher permeability was formulated. The existence of these regions was indicated by air flow measurements by Janssen (1997).

Roofs

Shankar and Hagentoft (2000) performed numerical calculations in order to predict the natural convection in horizontal roof structures. The Ra^* and Nusselt number were calculated given different insulation thicknesses and permeability of the insulation. It was found that an increase in insulation thickness, temperature difference and permeability of insulation material resulted in an increase in the natural convection and heat transfer. However, the calculations only included horizontally oriented insulation and the permeability was rather high ($>7.5 \cdot 10^{-9} m^2$).

Dyrbøl et al. (2002) performed measurements of convection in three different types of insulation. The test section was tested in both the vertical and horizontal position. A distinct convection-induced heat flux was found, even at material thicknesses as low as 200 mm and a temperature difference across the insulation of 20 K. Furthermore, the risk of convection increasing the total heat flow was found to be related to highly permeable insulation materials. Given a certain level of permeability, convection was able to increase the total heat flow by more than 3% even under the most ideal conditions and at small temperature differences. However, the mean temperature of the insulation was not kept constant which affects the thermal conductivity of the materials.

Wahlgren (2007) presented a thorough literature review studying natural and forced convection in horizontal attic insulation. The study found large differences in reported critical modified Rayleigh numbers and hence the onset of convection. Variations in constructions, material properties, workmanship and boundary conditions were highlighted as reasons for the large differences.

A thorough literature review of convection in highly insulated pitched roofs was conducted by Roels and Langmans (2016) highlighting the use of high-density insulation ($>20 kg/m^3$) and a continuous and wind tight vapour and wind barrier system in order to construct a well-performing and robust pitched wooden roof.

Convection and the effect on moisture transport

Natural convection in glass wool will not only affect the heat transmittance through the wall, but also cause moisture redistribution in walls (Geving and Uvsløkk, 2000; Langmans et al. 2012). The latter occurs when water vapour is transported by the air circulation inside the insulated cavities in the wall. Effects of natural and forced

convection on the hygrothermal performance of highly insulated building structures have been studied in laboratory measurements by Langmans et al. (2012), Kalamees and Kurnitski (2010) and Økland (1998). The results showed increased moisture levels at the upper cold part of the walls due to natural convection. It was also stated that an airtight vapour barrier on the warm side is required in order to obtain a moisture safe structure. However, roofs have not been part of these studies.

Objective and scope

The purpose of this study has been to investigate how the angle of inclination and the heat flow direction affect natural convection in thick timber frame structures with cavities filled with air permeable insulation.

Experimental work

Methods

Natural convection has been studied by laboratory measurements by use of a rotatable guarded Hot-Box. U-value and temperature distribution in the insulation have been measured on a timber frame structure with 500 mm thick cavities filled with battens of glass wool insulation. U-values are calculated on the bases of measured heat flow, metering area and temperature difference across the test section. The U-value is calculated according to NS-EN-ISO 8990 (1996) and based on the mean value of between 12 and 24 one-hour measurement periods. The metering area of the Hot-Box is 2450 mm·2450 mm. Surface thermal resistance coefficients were adjusted close to the standardized ones prior to the tests by adjusting the air flow velocities adjacent to the surface on both the hot and the cold sides. It is worth noting that during the measurements, the surface thermal resistances may differ slightly from the standardized values. Corrections to the values are made for these deviations so that all U-values are stated with normalized surface thermal resistance coefficients as specified in NS-EN-ISO 8990 (1996). The standardized conditions are interior surface thermal resistance, $R_{si} = 0.13 \text{ W/m}^2\text{K}$, and external surface resistance $R_{se} = 0.04 \text{ W/m}^2\text{K}$. The surface thermal resistances are kept constant for all the measurements.

Test section

The test section was composed of two timber frames of laminated wood. One frame had sills and studs of dimensions 48 mm·298 mm and one had sills and studs of dimensions 48 mm·198 mm, in sum 48 mm·496 mm. The two timber frames were fixed together using long construction screws and the longitudinal joint between the two timber frames was taped in order to avoid air leakages from one insulation cavity to another. Five of the screws were located within the metering area of the Hot-Box. The overall height of the test section was 2400 mm and the overall width was 3048 mm, see Figure 1. The test section had six vertical studs with centre-to-centre distance of 600 mm. The test section was insulated using glass wool insulation with a nominal heat conductivity of 0,035 W/mK and a density of 16 kg/m³. In total 4 layers of insulation was installed into the cavity; two layers of 150 mm, and two layers of 100 mm insulation. Gypsum boards with

a thickness of 12.5 mm were fixed on both the cold and warm sides of the timber frame test section.

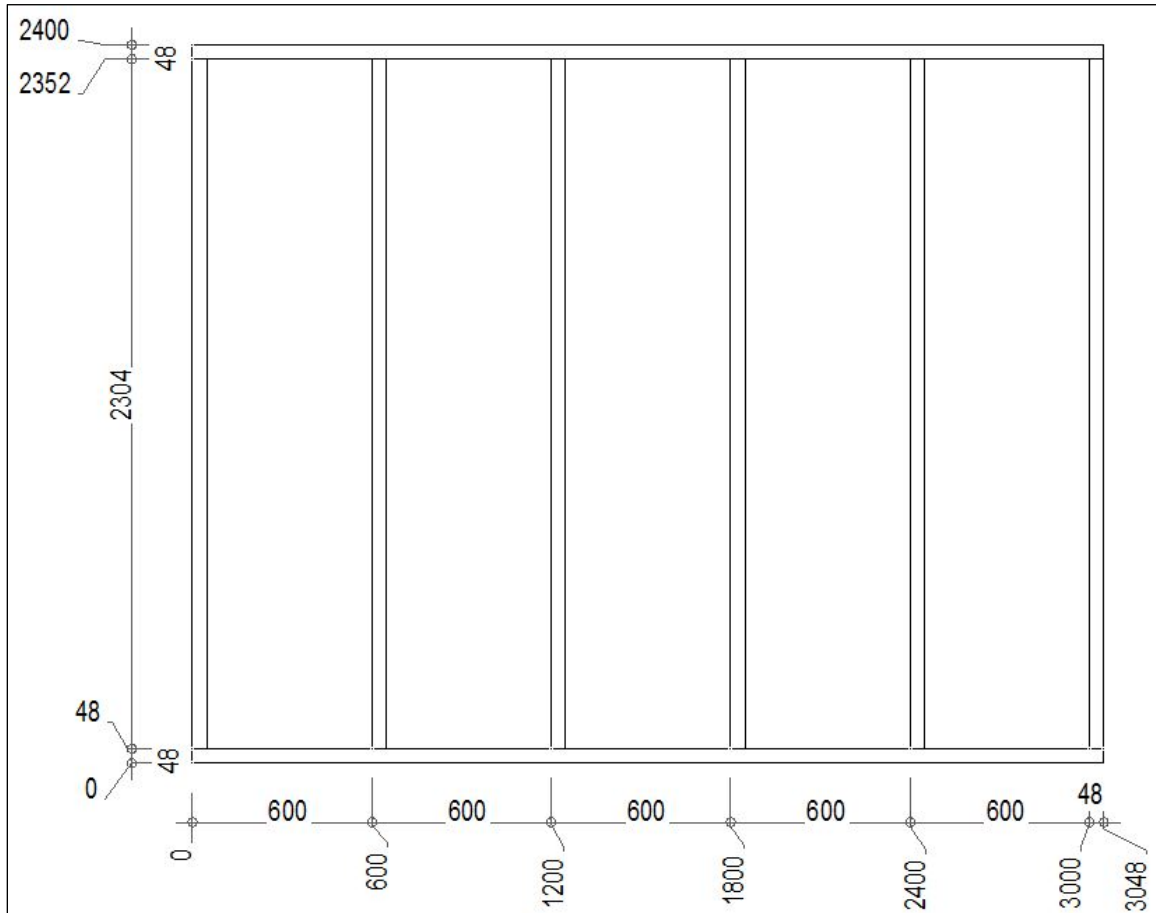


Figure 1. Cross-section of the timber frame test section. Dimensions in mm.

In order to study the effect of convection on the temperature profile, 39 thermocouples were installed inside and on the cold and warm sides of the test section. The thermocouples in the middle of the insulation layer were located 50, 100 and 150 mm away from the top and bottom sill as well as in the mid height of the wall, see Figure 2. The thermocouples were of type T. The frames in Figure 2 indicate thermocouples included in Figures 9–12.

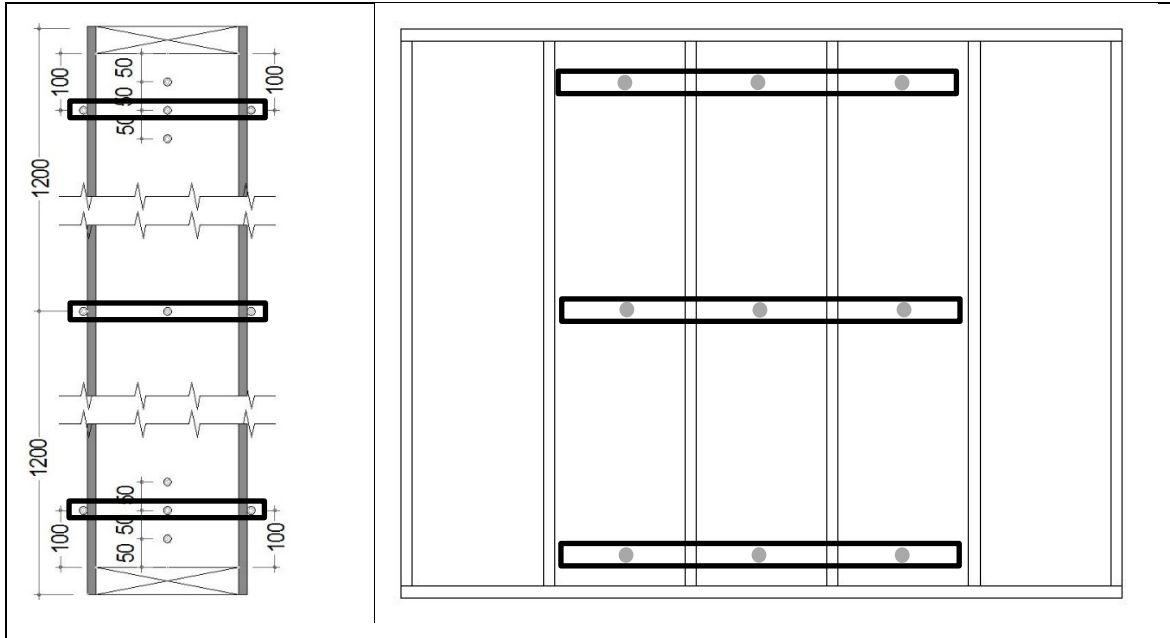


Figure 2. Positions of the 39 thermocouples, indicated by dots, inside (crosssection to the left) and on the cold and warm surfaces of the test section (elevation view to the right). Frames indicate the position of the thermocouples included in Figure 9-12.

Boundary conditions and test sequence

Natural convection is affected by several parameters. In this study, the angle of inclination, the heat flow direction and the temperature difference across the test section have been varied. The measurements were performed at a temperature difference of 20 and 40 K across the test section and a constant mean temperature of 10 °C. Measurements were performed with the test section in the following positions: wall, roof with pitch of 30° and 60° in addition to horizontal roof and floor. The tests were performed in steady-state conditions at temperature levels shown in Table 1. The test section was positioned between the hot and cold room of the guarded Hot-Box, as seen in Figure 3. In general, each test lasted for about 48 hours in order to achieve a measurement period of at least 12 hours with stable conditions.

Table 1 Overview of the variable tests and the conditions during the measurements.

Test variant	Angle of inclination [°]					Temperature cold room [°C]		Temperature warm room [°C]	
	90	60	30	0	180	0	-10	20	30
1	X					X		X	
2		X				X		X	
3			X			X		X	
4				X		X		X	
5					X	X		X	
6	X						X		X
7		X					X		X
8			X				X		X
9				X			X		X
10					X		X		X



Figure 3. The rotatable Hot-Box test facility. To the left, the test section is positioned as a floor (cold room below the test section). To the right, the angle of inclination of the test section is 30°.

Uncertainty assessment of Hot-Box measurements

Grynning et al. (2015) performed an assessment of the uncertainties associated with the Hot-Box measurements. The assessment was conducted with the identical Hot-Box as used in the current study. The assessment was performed according to the procedure described in NS-EN-ISO 12567-1 (2010). The uncertainties were stated with a coverage factor of two standard deviations and the corresponding 95% confidence interval. The uncertainty assessment of the current study is based on the work performed by Grynning et al. (2015).

As shown in equation 5 the root-mean-square (RMS) method is used to derive the uncertainty propagation of the measured U-value total uncertainty propagation $\frac{\Delta^P U_w}{U_w}$

$$\frac{\Delta^P U_w}{U_w} = \sqrt{\left[\frac{\Delta^P \Phi_w}{\Phi_w} \right]^2 + \left[\frac{\Delta^P A_w}{A_w} \right]^2 + \left[\frac{\Delta^P \delta \theta_{ie}}{\theta_{ie}} \right]^2} \quad (5)$$

$\frac{\Delta^P \Phi_w}{\Phi_w}$ is the uncertainty of the sample heat flow (W), $\frac{\Delta^P A_w}{A_w}$ is the uncertainty in the measurement area and $\frac{\Delta^P \delta \theta_{ie}}{\theta_{ie}}$ is the uncertainty in the temperature difference between the cold and sides of the Hot-Box.

The uncertainty of the sample heat flow is based on the heat balance equation of the test chamber. Uncertainty of $\frac{\Delta^P \Phi_w}{\Phi_w}$ is expressed in equation 6.

$$\frac{\Delta^P \Phi_w}{\Phi_w} = \sqrt{\left[\frac{\Delta^P \Phi_{IN}}{\Phi_w} \right]^2 + \left[\frac{\Delta^P \Phi_{EXTR}}{\Phi_w} \right]^2 + \left[\frac{\Delta^P \Phi_{FL,w}}{\Phi_w} \right]^2} \quad (6)$$

where $\frac{\Delta^P \Phi_{IN}}{\Phi_w}$ is the uncertainty in power input to metering chamber (W), $\frac{\Delta^P \Phi_{EXTR}}{\Phi_w}$ is the uncertainty of the metering chamber heat flows and $\frac{\Delta^P \Phi_{FL,w}}{\Phi_w}$ is the uncertainty in the test sample flanking heat loss (W).

No correlation between the various terms of the balance equation was found. By using a temperature reference bath, Grynning et al. (2015) found that the relative scattering in measured temperatures was lower than 0.02K.

Many uncertainties and systematic errors are avoided by conducting comparative measurements such as in this study. The test section is only inserted once into the Hot-Box apparatus. By comparing the results from different test conditions (angle and temperature), the uncertainties of metering area, heat conductivity of the materials and possible errors when inserting the test section into the apparatus are minimized. This is of course influencing the results of equation 5) and 6).

However rotating of the Hot-Box means introducing of some new uncertainties compared to the measurements performed by Grynning et al. (2015). First of all rotating of the Hot-Box introduces a possibility that the measurement chamber can move in relation to the test section. To control this the measurement chamber is equipped with actuators so that the position can be controlled outside the Hot-Box. Rotating of the Hot-Box also effects the surface thermal resistance. By measuring the temperature on both the

cold and warm surface of the test section in addition to the air temperature in the cold and warm chamber the interior surface thermal resistance and external surface resistance are measured.

Air permeability of the insulation material

Air permeability of the glass wool was measured according to NS-ISO 9053 (1993) using equation (2). The apparatus is shown in Figure 4. The air flow rate through the specimen is measured by use of a laminar flow meter. The air pressure difference across the test specimen is measured by use of a micromanometer. The glass wool specimens were sawn with a band saw to fit the apparatus. The specimens were conditioned in laboratory climate ($\sim 20\text{ }^{\circ}\text{C}$) and weighed before testing in order to calculate the density.

Three different test specimens both from the 150 mm insulation layer and 100 mm insulation layer were taken from two different insulation batts. The specimen dimension perpendicular to the flow direction was over-sized by 5 mm. Identical specimens were used to measure the permeability parallel and perpendicular to the fibre direction.

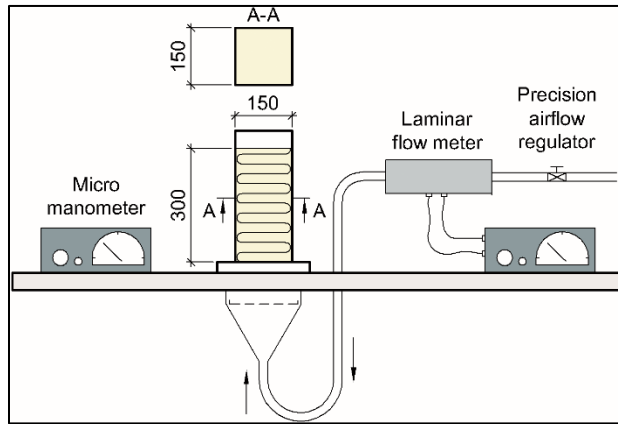


Figure 4. Principle of the apparatus used to measure the permeability of the glass wool.

Equivalent air permeability of the insulated cavities

In order to measure the air flow resistance of the insulated cavities of the test section, an airtight box was constructed. The box had a length of 600 mm, width of 500 mm and a height of 200 mm. In order to secure an evenly distributed air flow, a perforated steel sheet was placed perpendicular to the air flow in the middle of the box.

When measuring the practical air permeability of the test section, the bottom and top sills of the test section were dismantled. The box was fixed to each insulated cavity to measure air flow resistance through the insulated cavity, see Figure 5. The box was fixed to a pair of studs and the perimeter of the box was sealed to the test section. A rotameter was attached to the box in order to measure the air flow. In order to calculate the air flow resistance and an equivalent permeability, the pressure drop inside the cavities with glass wool insulation was measured, see Figure 5. The equivalent permeability was calculated according to equation 2). In cavity numbers 2, 3 and 4 from the left-hand image, the pressure difference was measured for a 500 mm centre-to-centre distance. This was done in order to examine whether the air flow resistance of the insulated cavities was evenly distributed through the cavity. In cavity 1 and 5, the

distance between the holes was 2000 mm. The pressure was measured at three different air flows: 5, 7 and 10 m³/h.

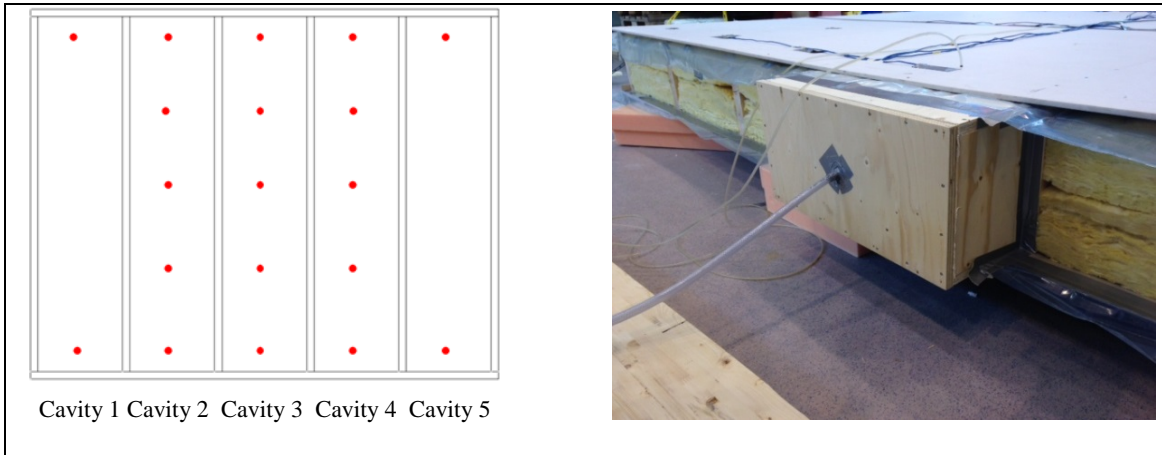


Figure 5. Equipment used for measuring equivalent air permeability of the insulated cavities of the test section. Red dots indicate positions of air pressure measurements. Test section seen from the cold side. I

Results

Hot-Box measurements

U-values derived from the Hot-Box measurements, surrounding conditions and the calculated modified Rayleigh number and Nusselt number for the different test variants are shown in Table 2. The modified Rayleigh number is calculated according to equations (1) and (3).

The Nusselt number is calculated by dividing each of the measured U-values by the measured U-value at a 180°-angle assuming that there is no convection in the insulated cavities when the test section is in a floor position with the heat flow direction downwards.

The Nusselt number is increasing rapidly with increasing Ra* for the 30° and 60° angles.

Table 2 Results from the Hot-Box measurements.

Test variant	Angle [°]	θ_e [°C]	θ_i [°C]	$\bar{\theta}$ [°C]	$\Delta\theta_{ie}$ [K]	U-value [W/m ² K]	Modified Rayleigh number [-]	Nusselt number [-]
1	90	0	20	10	20	0.0845±0.004	4.12	1.08±0.077
2	60	0	20	10	20	0.0836±0.004	4.12	1.06±0.076
3	30	0	20	10	20	0.0855±0.004	4.12	1.09±0.078
4	0	0	20	10	20	0.0848±0.004	4.12	1.08±0.072
5	180	0	20	10	20	0.0785±0.004	4.12	1.00±0.049
6	90	-10	30	10	40	0.0906±0.005	8.24	1.15±0.092
7	60	-10	30	10	40	0.1010±0.005	8.24	1.29±0.100
8	30	-10	30	10	40	0.1024±0.005	8.24	1.30±0.103
9	0	-10	30	10	40	0.0860±0.005	8.24	1.09±0.087
10	180	-10	30	10	40	0.0780±0.005	8.24	1.00±0.059

Permeability of the insulation material

Figure 6 shows the measured permeability of the 100 mm and 150 mm thick glass wool specimens as a function of the density of the glass wool. The average measured permeability perpendicular (\perp) and parallel (\parallel) to the main fibre direction was $1.62 \cdot 10^{-9} \text{m}^2$ and $4.25 \cdot 10^{-9} \text{m}^2$ respectively. The measured density of the different specimens varied from 16.3 to 19.0 kg/m³.

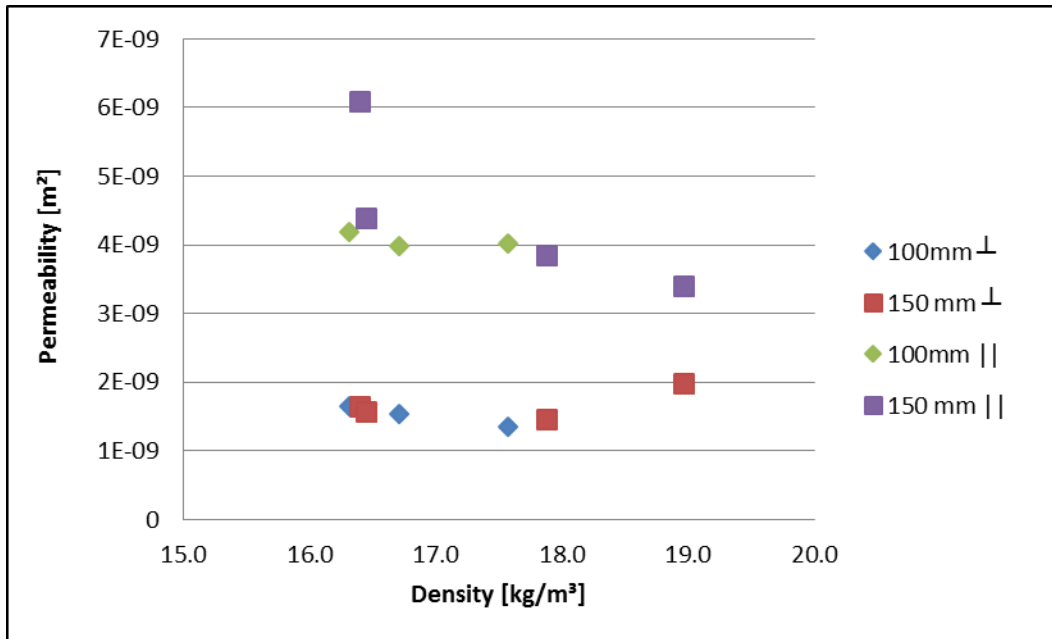


Figure 6. Permeability perpendicular and parallel to the main fibre direction as a function of the density of the glass wool specimen.

Measured equivalent permeability of the insulated cavities in the test section
 Figure 7 shows the results from the air flow resistance measurements of each of the five cavities in the test section. The equivalent permeability was calculated using equation (2). The average equivalent air permeability of the four cavities was $14 \cdot 10^{-9} \text{m}^2$.

In practise, with a total of four insulation layers, it is difficult to fill all the cavities precisely without any air gaps, as seen in Figure 8. The photo shows the bottom of the test section after the bottom beam has been removed. The tape which was used to seal the longitudinal joint in the bottom sill of the specimen was not removed before taking the picture.

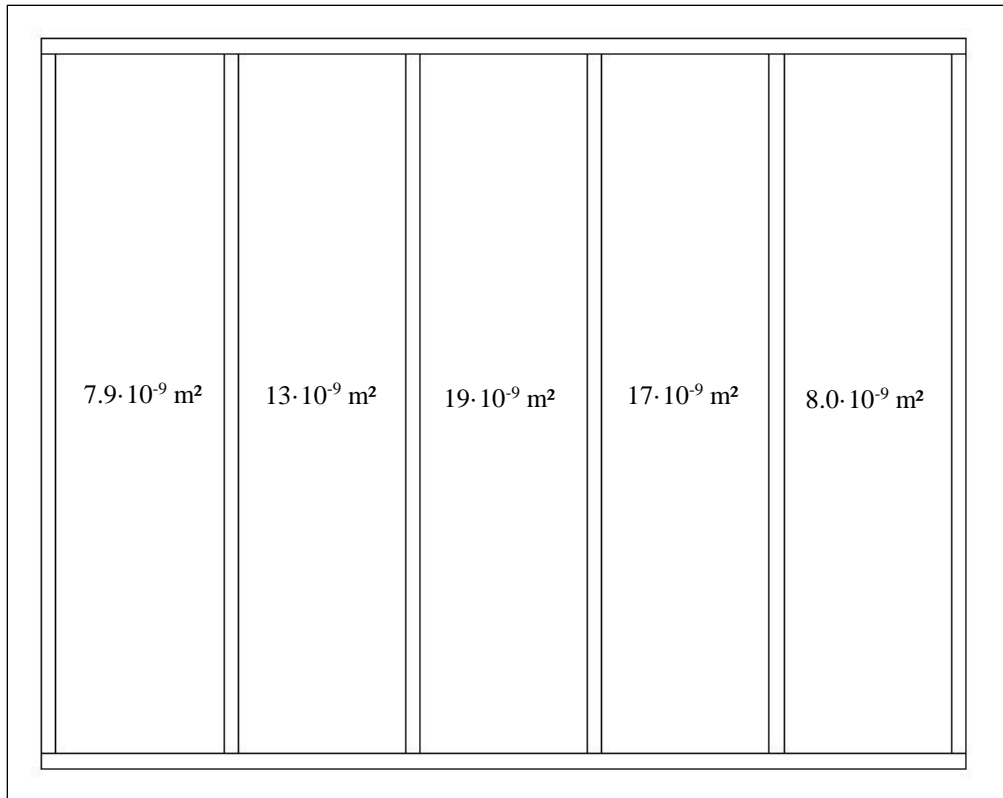


Figure 7. Measured equivalent permeability of the insulated cavities, test section seen from the warm side.



Figure 8. Air gaps in transition zones between the layers of insulation and between the insulation and the wood frame.

Temperature distribution through the insulation layers

Figures 9–12 show measured temperature profiles through the insulation layers in the three cavities, identified in Figure 2, at a temperature difference of 40 K across the test section. Figures 9–12 include three temperature profiles in each cavity. That means nine temperature profiles in total. Each profile consists of 24 hourly averaged values drawn on top of each other. The inclination of the test section is illustrated by a sectional drawing to the left. Only a range of the measurements is shown in this work. Temperature profiles that deviate from a straight line indicate convection in the insulation layer.

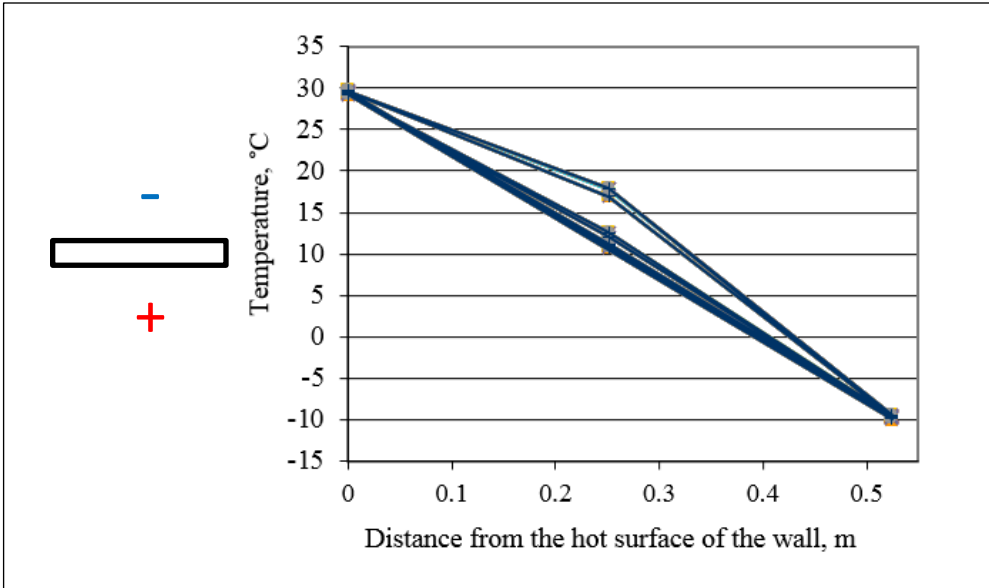


Figure 9. Temperature at the cold and warm surfaces of the test section and in the centre of the glass wool insulation, when oriented as a horizontal roof (see sectional drawing to the left)

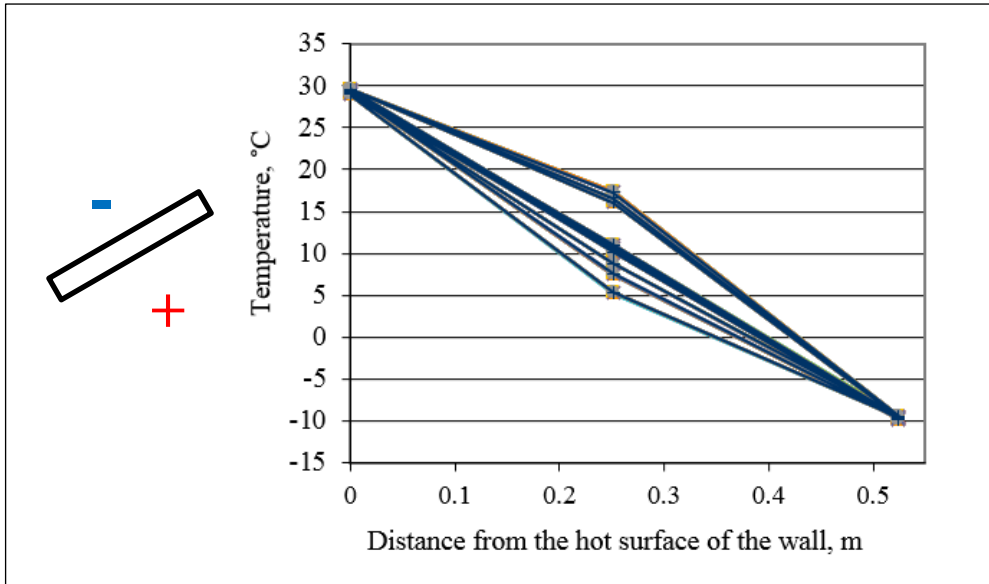


Figure 10. Temperature on the cold and warm surfaces of the test section and in the centre of the glass wool insulation at a 30-degree inclination (pitched roof).

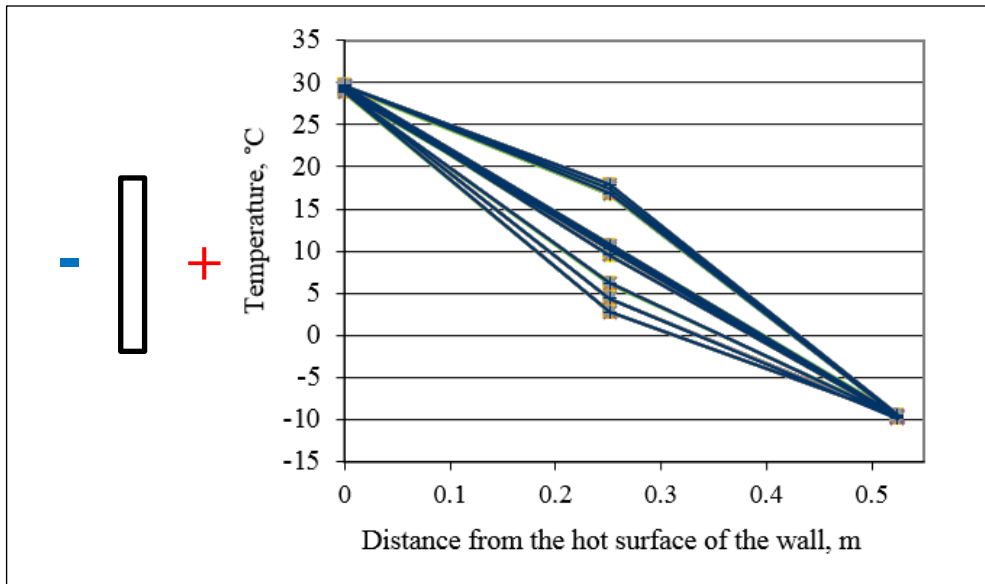


Figure 11. Temperature at the cold and warm surfaces of the test section and in the centre of the glass wool insulation, oriented as a wall

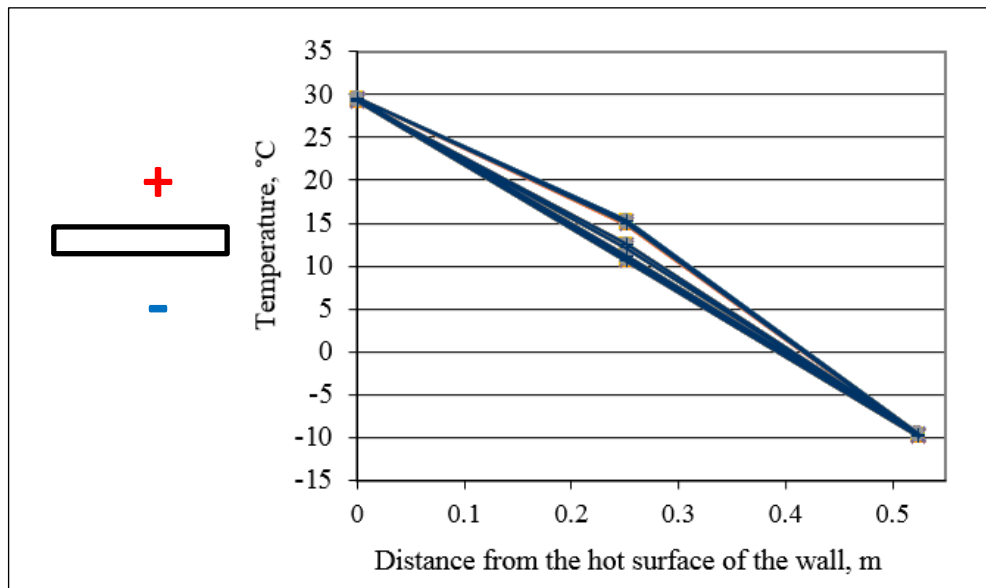


Figure 12. Temperature at the cold and warm surfaces of the test section and in the centre of the glass wool insulation, oriented as a floor

Discussion

Several laboratory studies have been performed prior to this study. However, these prior investigations have only included structures with insulation thicknesses up to 300 mm. A focus on energy efficiency in the building stock have made the building sector move towards more insulated structures. Therefore, it is highly relevant for the construction

industry to increase its knowledge about convection in highly insulated structures, e.g. > 300 mm insulation thickness.

Angle of inclination

Given a temperature difference of 20 K, the Nusselt number is approximately equal for the angles 90°, 30° and 0°. By increasing the temperature difference to 40 K, the Nusselt number increases for all angles except for the horizontal roof configuration. Angles of 30° and 60° and a temperature difference of 40 K give the highest Nusselt number, showing that the pitched roof configuration gives the highest U-values for the test section. For the 30- and 60-degree inclinations, there is an approximately 25 % increase in the Nusselt number when the temperature difference increases from 20 to 40 K.

According to NS-EN ISO 10456 (2007), natural convection can be neglected if $Ra^* < 2.5$. The results from the present study, given an insulation thickness of 500 mm, are in line with this. Previous studies by Bankvall (1972) indicate that there will be no convection in wall structures with Ra^* below 6 when the ratio is 5 between height and thickness of the cavities. The results of the present study show that a Ra^* of 4 gives significant convection for all angles except for the floor configuration. Measurements performed by Uvsløkk (2010) on a timber frame wall with 300 mm glass wool insulation showed convection for Ra^* of 3.7. A literature review performed by Wahlgren (2007) shows that previous studies indicate no convection for a Ra^* below 10-30 for the horizontal roof configuration. The present study of a timber frame structure with an insulation thickness of 500 mm shows that the onset of convection occurs at a lower Ra^* than the previous studies have shown. The main reason for this is most likely imperfections in the insulation layer in real timber frame structures giving a lower flow resistance than indicated by the permeability measurements of the insulation material.

Temperature difference over the test section

The results show that an increased temperature difference results in increased convection and hence increased practical U-values for the timber frame structures. The effect is largest for pitched roofs and wall configurations. The average temperature has been kept constant in the present study. Janssen (1997) calculated a Nusselt number between 1.07 and 1.12 based on Hot-Box measurements on a full-size (2400 mm·3048 mm) timber frame wall with 200 mm glass wool insulation dependent on the temperature difference over the wall. For a timber frame wall with 300 mm glass wool, the Nusselt number varied between 1.04 and 1.14. Janssen's measurements were carried out in the same Hot-Box apparatus as used in the present study. The calculated Nusselt numbers based on measurements from the present study of a timber frame structure with 500 mm glass wool varied from 1.08 ($\Delta\theta_{ie} = 20$) to 1.15 ($\Delta\theta_{ie} = 40$). The results of the study are in line with the former studies performed by Janssen (1997) and Uvsløkk (1996, 2000).

Given a horizontal roof structure and a permeability for the insulation material of $7.5 \cdot 10^{-9} \text{ m}^2$, the calculations of Shankar and Hagentoft (2000) give a Nusselt number of approximately 1.3 for an insulation thickness of 500 mm and a temperature difference of 40 K. The comparable measured Nusselt number of the present study is 1.09. The permeability of the glass wool used in this study was respectively $1.62 \cdot 10^{-9} \text{ m}^2$ and $4.25 \cdot 10^{-9} \text{ m}^2$ for glass wool perpendicular and parallel to the main fibre direction. It is difficult to compare the results when the permeabilities are so different. However, the

rather large difference in the calculated and measured Nusselt number shows that low permeability is favourable considering natural convection.

The present study also shows a big increase in the Nusselt number for the 30- and 60-degree inclinations when the temperature difference is raised from 20 to 40 K. A possible explanation is that an increased temperature difference and a larger driving force implies formation of more convection loops inside the test section. However, formation of such loops cannot be seen from the temperature profiles in Figure 10.

Permeability of insulation material

The permeability is approximately twice as large parallel to the main fibre direction compared to when it is perpendicular to the main fibre direction. The measured permeability of the insulation material perpendicular and parallel to the main fibre direction was $1.62 \cdot 10^{-9} \text{m}^2$ and $4.25 \cdot 10^{-9} \text{m}^2$ respectively for glass wool specimens from the same batch as used in the test section. This is in line with previous results from Økland (1998) and Dyrbøl et al. (2002). Uvsløkk et al. (2010) measured a permeability of $2.5 \cdot 10^{-9} \text{m}^2$ and $5.1 \cdot 10^{-9} \text{m}^2$ perpendicular and parallel to the main fibre direction respectively. The higher permeability can be explained by a lower density of the glass wool of 13.2 kg/m^3 . Generally, the permeability measurements performed in the present study shows approximately 10% greater permeability for the 150 mm batts compared to the 100 mm batts. The results cannot be explained by difference in density of the insulation. One main reason for the difference is that the 100 mm insulation was installed in three layers, while the 150 mm insulation was installed in two layers in the test apparatus. This could imply some differences in the installation of the specimens. Three layers of insulation also imply a possible lower permeability because of the surface resistance of the glass wool.

Equivalent permeability of insulated cavities

The average equivalent permeability, calculated on the basis of the air flow and pressure gradient measurements in the insulated cavities of the test section, was $14 \cdot 10^{-9} \text{m}^2$. This is nearly ten times larger than the measured permeability of the insulation material samples. This average equivalent permeability cannot be used for accurate estimation of Ra^* , but gives a good indication on the deviation between theoretical and practical flow resistance in insulated cavities. Note that there is a factor two ratio between the smallest and the largest equivalent air permeability numbers of the insulation cavities. Cavity 1 and 5 has considerable lower permeability compared to cavity 2, 3 and 4. A likely explanation is differences in workmanship. As Figure 8 shows, there are some air gaps in the transition zones between the insulation layers and between the insulation and the timber frame. Large insulation thickness often means that for practical reasons, the insulation must be installed in several layers within the structure. This implies more transition zones and higher risk of imperfections and increased equivalent permeability of the insulated cavities. Even when the insulation is carefully installed as done in the experiments, there might be imperfections in transition zones between the insulation and the timber frame and between the different layers of insulation. In practice, with a total of four insulation layers, it is difficult to fill all the cavities precisely, as seen in Figure 8.

The air flow due to natural convection appears primarily in the zones near the cladding board on the exterior and interior sides of the test section where the pressure

gradients are largest. Air gaps near the surfaces of the test section will increase the risk of convection while air gaps in the middle of the insulation will affect the natural convection to a smaller extent, because of smaller driving forces.

Temperature profiles

The temperature profiles clearly show convection in the pitched roof and wall positions. In the floor situation, there is theoretically no potential for convection. Figure 12 shows the temperature profiles when there is no convection. As Figure 12 shows, there is some dissipation in the diagram, including where there is no theoretical potential for convection. When the insulation thickness is 500 mm, accurate positioning of the thermocouples in the middle of the insulation is challenging and a likely explanation is inaccurate positioning of the thermocouples.

Recommendations and measures to reduce the risk of convection

For practical application natural convection can be reduced by dividing the insulation layer with a vapour open convection barrier. Using this approach, the temperature gradient is reduced thus lowering the driving force.

Conclusion

Both the temperature difference across the test section and the angle of inclination of the test section affect the convection in the insulated cavities giving increased U-values and Nusselt numbers. Also, measured temperature profiles inside the insulation cavity clearly show convection in the test section for the pitched roof and wall configurations. For practical application, an efficient measure to reduce the natural convection is to divide the insulation layer into two thinner layers by using a vapour open convection barrier for walls and roof structures. Even though the insulation was carefully installed insulation mistakes was discovered. The authors recommend use of a convection barrier in both wall and pitched roof structures if the insulation thickness exceeds 200 mm. A convection barrier will also reduce the impact of mistakes in the insulation. The use of a convection barrier is by that a simple means to reduce the risk of moisture problems and heat loss from a structure and thereby the energy use of buildings during operation.

References

- Bankvall, C. (1972) *Natural convective heat transfer in insulated structures, Report 38*. Division of Building and Technology, Lund Institute of Technology, Sweden.
- Bjerkevoll, G.O. (1994) Hot-Box målinger på høyisolerte bygningskonstruksjoner (Hot-Box measurements on highly insulated building constructions). *Hovedoppgave NTH*, Trondheim (In Norwegian).
- Brown, W. C., Bomberg, M. T., Ullett, J. M. & Rasmussen, J. (1993) Measured thermal resistance of frame walls with defects in the installation of mineral fibre insulation, *Journal of Thermal Insulation and Building Envelopes* 16: 318–339.
- Dyrbøl, S., Svendsen, S. & Elmroth, A. (2002) Experimental Investigation of the Effect of Natural Convection on Heat Transfer in Mineral Wool. *Journal of Building Physics* 26: 153–164.

- Geving, S. (2011) *Fuktskader Årsaker, Utbedringer og tiltak (Moisture damage, causes, repair)*, SINTEF Byggforsk, Oslo, Norway, ISBN: 978-82-536-1228-7 (In Norwegian).
- Geving, S. & Uvsløkk, S. (2000) Moisture conditions in timber frame roof and wall structures. *Project report 273*. Norwegian Building Research Institute, Oslo, Norway
- Grynning, S., Misiwopecki, C., Uvsløkk, S., Time, B. & Gustavsen, A. (2015) Thermal performance of in-between shading systems in multilayer glazing units: Hot-box measurements and numerical simulations. *Journal of Building Physics* 39: 147–169.
- Gullbrekken, L., Geving, S., Time, B., Holme, J. & Andresen, I. (2015) Moisture conditions in well-insulated wood-frame walls. Simulations, laboratory measurements and field measurements. *Wood Material Science & Engineering*
- Janssen, H. (1997) Thermal performance of highly insulated wood frame walls. *Master's Thesis KUL NTNU*, Trondheim.
- Johannessen, E. (1995) Hot-Box målinger på høysisolerte bygningskonstruksjoner. (Hot-Box measurements on highly insulated building constructions). *Hovedoppgave NTH*, Trondheim (In Norwegian).
- Jordanger, G.O. (1995) Naturlig konveksjon i vegger laboratorieforsøk. (Natural convection in walls laboratory measurements). *Hovedoppgave NTH*, Trondheim (In Norwegian).
- Kalamees, T. & Kurnitski, J. (2010) Moisture Convection Performance of External Walls and Roofs. *Journal of Building Physics* 33: 225–247.
- Langmans, J., Klein, R. & Roels, S. (2012) Hygrothermal risks of using exterior air barrier systems for highly insulated light weight walls: A laboratory investigation. *Building and Environment* 56: 192–202.
- Lecompte, J. (1990) The influence of natural convection on the thermal quality of insulated cavity construction. *Building Research and Practice* 6: 346–354.
- Marmolet, L., Lewandowski, M. & Perwuelz, A. (2012) An Air Permeability Study of Anisotropic Glass Wool Fibrous Products. *Transport in Porous Media* 93: 79–97.
- NS-EN-ISO 8990 (1996) *Thermal insulation – Determination of steady-state thermal transmission properties – Calibrated and guarded hot box*, Standard Norge, Norway
- NS-EN-ISO 12567-1 (2010) *Thermal performance of windows and doors Determination of thermal transmittance by the hot-box method Part 1: Complete windows and doors*, Standard Norge, Norway
- NS-EN ISO 10456 (2007) *Hygrothermal properties – Tabulated design values and procedures for determining declared and design thermal values*, Standard Norge, Norway.
- NS-ISO 9053 (1993) *Acoustics materials for acoustical applications Determination of airflow resistance*, Standard Norge, Norway.
- Roels, S. & Langmans, J. (2016) Highly insulated pitched roofs resilient to air flow patterns: guidelines based on a literature review, *Energy and Buildings* <http://dx.doi.org/10.1016/j.enbuild.2016.03.071>.

- Shankar, V. & Hagentoft, C.E. (2000) A Numerical Study of Effect of Natural Convection on Thermal Properties of Horizontal Oriented Porous Insulation. *Journal of Building Physics* 24: 155–167.
- Uvsløkk, S., Skogstad, H.B. & Aske, I.J. (1996) Natural convection in timber frame walls with thick thermal insulation layer. *Nordic Building Physics Conference*, Espoo, Finland.
- Uvsløkk, S., Skogstad, H.B. & Grynning, S. (2010) How to prevent natural convection causing extra heat loss and moisture problems in thick insulation layers. *3rd Nordic Passive House Conference*, Aalborg, Denmark.
- Wahlgren, P. (2007) Overview and Literature Survey of Natural and Forced Convection in Attic Insulation. *Journal of Building Physics* 30: 351–370.
- Økland, Ø. (1998) Convection in Highly-Insulated Building Structures. Department of Civil and Transport Engineering. Doctoral Thesis 1998:86 NTNU, Trondheim, Norway.